

# Collective Granular Dynamics in a Shaken Container at Low Gravity Conditions

J. E. Kollmer, A. Sack, M. Heckel, F. Zimmer, P. Mueller, M. N. Bannerman and T. Pöschel

*Friedrich-Alexander Universität Erlangen-Nürnberg, Institute for Multiscale Simulation, Erlangen, Germany*

**Abstract.** We investigate the collective dissipative behavior of a model granular material (steel beads) when subjected to vibration. To this end, we study the attenuation of the amplitude of an oscillating leaf spring whose free end carries a rectangular box partly filled with granulate. To eliminate the perturbing influence of gravity, the experiment was performed under conditions of microgravity during parabolic flights. Different regimes of excitation could be distinguished, namely, a gas-like state of disordered particle motion and a state where the particles slosh back and forth between the container walls in a collective way, referred to as *collect-and-collide* regime. For the latter regime, we provide an expression for the container size leading to maximal dissipation of energy, that also marks the transition to the gas like regime. Also for systems driven at fixed amplitude and frequency, we find both the gas regime and the *collect-and-collide* regime resulting in similar dissipative behavior as in the case of the attenuating vibration.

**Keywords:** Granular material, damping

**PACS:** Granular systems, classical mechanics of: 45.70.-n,

## INTRODUCTION

The characteristic property of dynamic granular systems, when compared to other many-particle systems, is their ability to dissipate mechanical energy through particle collisions. While the dissipative properties of vibrated granulate have long been investigated [1, 2], recently a large body of literature [3, 4, 5, 6, 7] has emerged on the mechanics and technical application of this damping mechanism in the form of *granular dampers*. A granular damper is a container partly filled by granular particles which may be attached to vibrating machinery to attenuate the amplitude of the oscillations. In its regime of operation, the granular material's dynamics are determined primarily by the inter-particle and particle-wall collisions rather than by long-lasting sliding contacts between the grains. Saluena et al. [1] and Opsomer et al. [8] have shown that several regimes of energy dissipation exist for a granular damper and that the transitions between these regimes are determined primarily by the influence of gravity. An efficient operation of a granular damper can only be expected if the average kinetic energy of the particles is much larger than their average potential energy (the damper operates in the *dynamic or collisional* regime). Therefore, in order to carefully investigate this regime, the influence of gravity must be minimized. This can either be achieved using strong accelerations or by performing the experimental investigations under conditions of weightlessness. In this proceeding we compare the experimentally observed attenuation of an oscillating spring by a granular damper under mi-

crogravity conditions to an effective model for the energy dissipation of a granular damper operating in the *collect-and-collide* regime [9]. A formula to optimize granular dampers and explaining the limits of *collect-and-collide* is derived and validated. We also present experimental results for a steadily driven system showing that our findings are not limited to attenuated oscillators [10].

## EXPERIMENT

Our experimental setup consists of a rectangular polycarbonate box of adjustable length that is partially filled with steel beads and attached to the top end of a spring blade (see Fig. 1) and detailed in [9]. The internal dimensions of the container are  $50\text{ mm} \times 50\text{ mm} \times L$ , where the length  $L$  (in the direction of the oscillation) is adjusted by altering the spacing of the end walls. The walls have a thickness of 5 mm and the container's net weight (without granulate) is  $M = 434\text{ g}$ . Four different container lengths of  $L = 40, 65, 85,$  and  $104\text{ mm}$  are used. The box is loaded with  $N = 37$  precision steel ball-bearings of diameter  $\sigma = 10\text{ mm}$  and mass  $m = 4.04\text{ g}$ . The initial deflection of the spring,  $A_0$ , is  $10.7\text{ cm}$ .

The motion of the box and the contained particles is recorded using a high speed camera (see Fig. 2). The position of the damper and the center of gravity of the particles are tracked from the top-view. To assure conditions of weightlessness, the experiment is performed in the low gravity environment achieved on a parabolic flight.

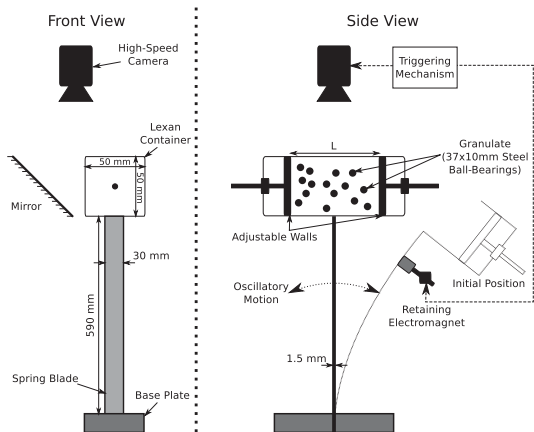


**FIGURE 1.** Schematic of the experimental setup in front view (left) and side view (right). The curvature of the oscillations is exaggerated for the purpose of illustration.

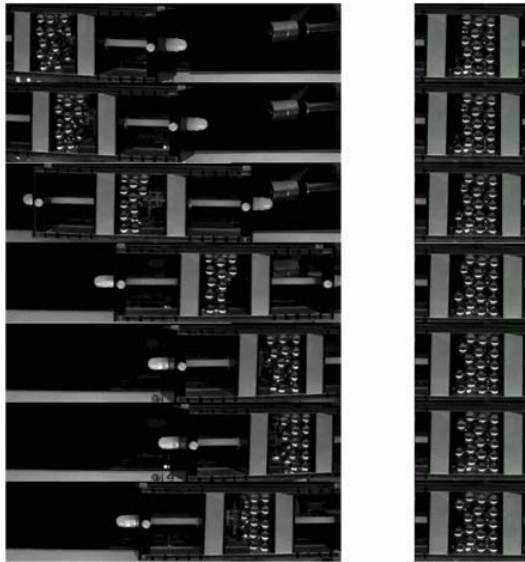


**FIGURE 2.** Frames from the high speed camera: *Collect-and-collide* behavior when the oscillation has a large amplitude (left) and unordered motion after the amplitude has declined below a threshold (right) in the  $L = 40$  mm sample. The frames are ordered so that time progresses downwards.

The experiment is numerically simulated in DYNAMO [11], an event driven DEM software. The model assumes a 1D oscillation, no air resistance, ideal spring, hard and frictionless spheres as well as instantaneous collisions [9]. All other parameters (unless otherwise noted) are kept in accordance to the experiment.

## RESULTS

The positions of the damper  $x_{\text{Box}}$  and center of gravity of the particles  $x_{\text{COM}}$  are experimentally measured as a function of time for four different box lengths  $L$ . In Fig. 3 two experimental measurements for  $L = 40$  mm are reported and both are in close agreement. We use this data set to determine the coefficients of restitution for particle-particle collisions,  $\epsilon_{pp} = 0.75$  and particle-wall collisions  $\epsilon_{pw} = 0.76$ , so that the simulation is in excellent agreement with the experimental results. Keeping the model parameters fixed the numerical simulation is performed for several different box lengths and compared with the corresponding experimental data (see Figs. 4).

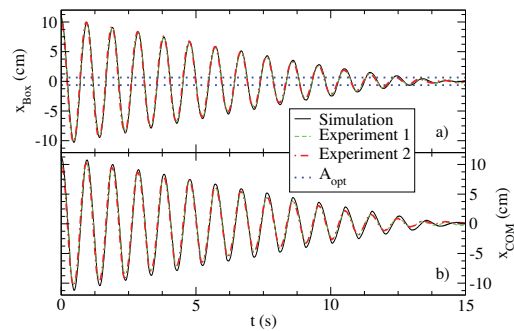


**FIGURE 3.** A comparison of simulation results and experimental data for (a) the box position  $x_{\text{Box}}$  and (b) the granulate center of mass  $x_{\text{COM}}$  as a function of time for a box length of  $L = 40$  mm. The simulation data is fitted to the experimental data through the coefficients of restitution. The dashed blue line ( $A_{\text{opt}}$ ) is discussed later in the text.

In general, the simulation results are in excellent agreement with the models predictions. This implies that the approximations of the model (1D oscillations, no air resistance, ideal spring) are small and have little effect on the dynamics of the granular damper. Some of these approximations may already be compensated for in the fitting of the coefficients of restitution, but they appear to be well behaved with the changes in box length.

In the high-speed-recordings as well as in the simulation we see the particles in the so called *collect-and-collide* regime where all particles are collected onto the inward moving wall until the inflection point where the wall will start to decelerate. The particles, as a bulk, get released and travel straight ahead to impact with the opposite wall and get collected there.

We observe a stronger damping for increasing  $L$ . Since this cannot hold true for arbitrary large boxes, we postulate the existence of an optimal box length  $L_{\text{opt}}$ .

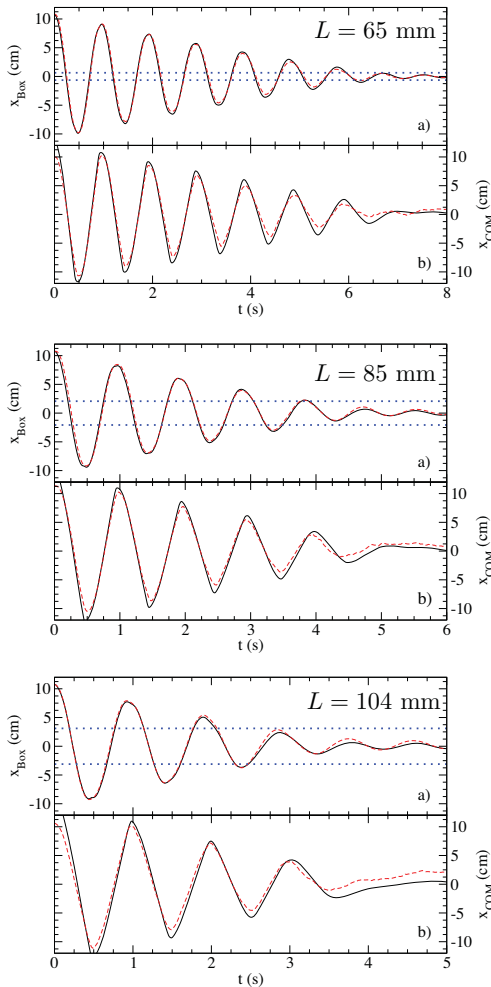


**FIGURE 4.** A comparison of simulation results and experimental data at the box length of  $L = 65$  mm,  $L = 85$  mm and  $L = 104$  mm: (a) the box position  $x_{\text{Box}}$  and (b) the granulate center of mass  $x_{\text{COM}}$  as a function of time. Line types are described in Fig. 3. The simulation data is not fitted to this data set and the parameters of Fig. 3 are used. Note the change of timescale.

## OPTIMAL DAMPING

In the *collect-and-collide* regime we can find an analytic expression for optimal damping. The relative velocity of granulate and box must reach a maximum at the time of collision. The centre of mass velocity of the granulate at the end of the inward part of the first stroke is assumed to be, on average, the maximum plate velocity at the

center of the oscillation length. The optimal box length for a given initial amplitude  $A_0$  of oscillation can then be estimated from intersecting the straight motion of the particles with the harmonic motion of the wall. The resulting optimal box length,  $L_{\text{opt}}$ , maximizes the relative impact velocity for a given  $A_0$  [9]:

$$L_{\text{opt}} = \pi A_0 \sqrt{\frac{M}{M + Nm}} + \sigma_{\text{layer}}, \quad (1)$$

with  $\sigma_{\text{layer}}$  being the length of the container that is occupied by the collapsed particles. The optimal box length for the system studied is predicted to be  $L_{\text{opt}} = 311$  mm. A simulation performed at this optimal box length (Figure 5) displays very high damping when compared to the shorter box lengths.

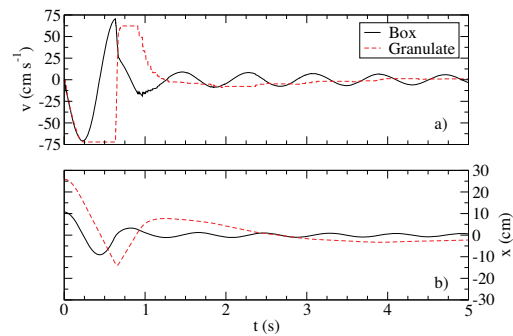


**FIGURE 5.** Simulation results for the box and granulate (a) velocity and (b) position as a function of time for the optimal box length of  $L = 311$  mm. Almost all energy is lost during the first impact.

For  $L = L_{\text{opt}}$  the *collect-and-collide* behavior stops after the first collision. Reordering Eq. (1) reveals that systems with decaying amplitude and  $L < L_{\text{opt}}$  will eventually reach an amplitude of optimal damping  $A_{\text{opt}}$  given by:

$$A_{\text{opt}} = \frac{L - \sigma_{\text{layer}}}{\pi \sqrt{\frac{M}{M + Nm}}} \quad (2)$$

We mark  $A_{\text{opt}}$  as blue dotted lines in Figs. 3 and 4. As can be seen in these figures, once  $A(t)$  drops below  $A_{\text{opt}}$  the grains ( $x_{\text{COM}}$ ) dissipated most of their kinetic energy and no longer perform the well ordered *collect-and-collide* motion.

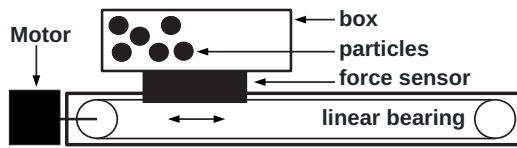


**FIGURE 6.** Sketch of the experimental setup of the driven system.

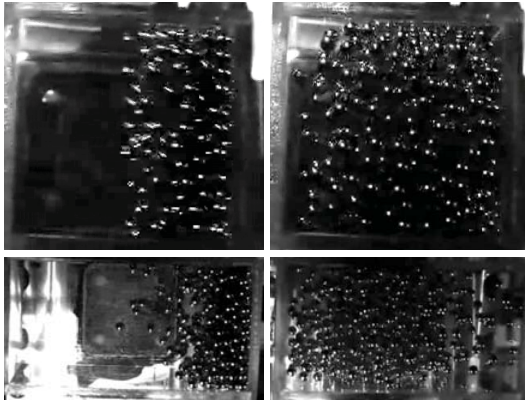


**FIGURE 7.** *Collect-and-collide* behavior in a 50 mm box (top left) and a 100 mm box (bottom left) shaken at an amplitude  $> A_{opt}$  and unordered particle motion in the 50 mm box (top right) and 100 mm box (bottom right) at a shaking amplitude  $< A_{opt}$ . The large box contains 473 and the small box 507 steel beads with a diameter of 4 mm.

## STEADY STATE CONDITIONS

So far we considered only an attenuated system with decaying amplitude. To test whether the observed behavior (*collect-and-collide*,  $L_{opt}$ ) is also applicable for steady state systems we employ another experiment: We replace the spring by a linear driver and subject the box containing a number of grains to sinusoidal driving of fixed amplitude and frequency. Figure 6 is a sketch of the experimental setup.

As can be seen from Fig. 7 the *collect-and-collide* regime is observed for  $A > A_{opt}$  while for  $A < A_{opt}$  we find the particles in a disordered, gas like, motion. This can be understood since, for  $A < A_{opt}$  the wall cannot collect the particles as they would impact a wall accelerating away from them.

We have seen that a simple (hard spheres, no friction, no air) model can describe the behavior of a granular damper attenuating an oscillating system. Assuming the grains moving as a bulk the optimal length for a granular damper can be given by an analytic expression. The *collect-and-collide* behavior ceases for amplitudes below

a given threshold which is related to the optimal damping length. Further experiments confirm that the observed behavior holds also true for steadily driven systems [10].

## ACKNOWLEDGMENTS

We thank the German Science Foundation (DFG) for funding via the grant FOR608 and through the Cluster of Excellence “Engineering of Advanced Materials” as well as the German Aerospace Center (DLR) and the European Space Agency (ESA) for funding the parabolic flight campaigns.

## REFERENCES

1. C. Salueña, S. Esipov, T. Pöschel, and S. Simonian, “Dissipative properties of granular ensembles,” in *Proceedings of SPIE - The International Society for Optical Engineering. Smart Structures and Material: Passive Damping and Isolation*, 3327, San Diego, CA, 1998, pp. 23–29.
2. C. Salueña, T. Pöschel, and S. E. Esipov, *Phys. Rev. E* **59**, 4422–4425 (1999).
3. K. Mao, M. Y. Wang, Z. Xu, and T. Chen, *Powder Tech.* **142**, 154–165 (2004).
4. T. Chen, K. Mao, X. Huang, and M. Y. Wang, “Dissipation mechanisms of nonobstructive particle damping using discrete element method,” in *Proceedings of SPIE - The International Society for Optical Engineering. Smart Structures and Material: Damping and Isolation*, edited by D. J. Inman, Newport Beach, CA, 2001, vol. 4331, pp. 294–301.
5. X.-M. Bai, B. Shah, L. M. Keer, Q. J. Wang, and R. Q. Snurr, *Powder Tech.* **189**, 115–125 (2009).
6. X.-M. Bai, L. M. Keer, Q. J. Wang, and R. Q. Snurr, *Gran. Mat.* **11**, 417–429 (2009).
7. M. Sánchez, and L. A. Pugnaloni, *J. Sound Vib.* **330**, 5812–5819 (2011).
8. E. Opsomer, F. Ludewig, and N. Vandewalle, *Phys. Rev. E* **84**, 051306 (2011).
9. M. N. Bannerman, J. E. Kollmer, A. Sack, M. Heckel, P. Müller, and T. Pöschel, *Phys. Rev. E* **84**, 011301 (2011).
10. A. Sack, M. Heckel, F. Zimmer, J. E. Kollmer, and T. Pöschel, (*submitted*) (2013).
11. M. N. Bannerman, R. Sargant, and L. Lue, *J. Comp. Chem.* **32**, 3329–3338 (2011).